International Journal of Innovative Engineering Applications

Journal homepage: https://dergipark.org.tr/ijiea

CFD ANALYSIS OF AN AIRCRAFT TURBOFAN ENGINE COMBUSTION PROCESS AND THE EFFECT ON TURBINE

***İbrahim Can*[1], *Doğan Engin Alnak*[2], *Muhammed Sipahi*[*1]**

[1]*Sivas Cumhuriyet Üniversitesi Fen Bilimleri Enstitüsü Savunma Sanayi Teknolojileri ve Stratejileri ABD, Sivas, Türkiye*
[2]*Sivas Cumhuriyet Üniversitesi Teknoloji Fakültesi, İmalat Mühendisliği Bölümü, Enerji Sistemleri ABD, Sivas, Türkiye*

Abstract

Original scientific paper

In this paper, a two-dimensional computational fluid dynamics (CFD) study of turbofan engine is presented using (ANSYS) Fluent Program, the Navier–Stokes equations is used for analysis, including a two-dimensional and symmetrical drawing of both the combustion chamber and in a 1.5 stage axial flow turbine. A General Electric (GE)-90 turbofan engine nacelle was used with National Advisory Committee Of Aeronautics (NACA) 63-412 type blades were used for the analysis of the flow on the turbine blades. Combustion chamber simulations were carried out using a previous study. The computational results were compared with other studies on the exergetic analysis of a GE-21 turbojet engine. The GE-21 engine had a combustion chamber temperature of 2900 K, while the GE-90 engine had a temperature of around 2706 K. The previous study considered the velocity of fluid flow to be 200 m/s, whereas the velocity of flow in this study was 209 m/s as determined in the part of analysis and result.

Keywords: *Turbine blade, CFD, combustion chamber, ANSYS.*

BİR UÇAK TURBOFAN MOTORUNUN YANMA SÜRECİ VE TÜRBİN ÜZERİNE ETKİSİNİN HAD ANALİZİ

Özet

Orijinal bilimsel makale

Bu makalede, ANSYS Fluent Programı kullanılarak, hem yanma odasının hem de 1.5 kademeli eksenel akış türbininin iki boyutlu ve simetrik çizimini içeren turbofan motorunun iki boyutlu hesaplamalı akışkanlar dinamiği (HAD) çalışması sunulmaktadır. Türbin kanatlarındaki akışın analizi için NACA 63-412 tipi kanatlı GE-90 turbofan motor nasel kullanılmıştır. Yanma odası simülasyonları, önceki bir çalışma kullanılarak gerçekleştirilmiştir. Hesaplama sonuçları, bir GE-21 turbojet motorunun ekserjetik analizine ilişkin diğer çalışmalarla karşılaştırıldı. GE-21 motorunun yanma odası sıcaklığı 2900 K, GE-90 motorunun sıcaklığı ise 2706 K civarındaydı. Önceki çalışmada, sıvı akış hızı 200 m/s olarak düşünülmüş, oysaki son çalışmada sıvı akış hızı 209 m/s olarak tespit edilmiştir.

Anahtar Kelimeler: *Türbin kanadı, HAD, yanma odası, ANSYS.*

1 Introduction

In recent years many computational and experimental studies have been conducted in order to obtain the best efficiency for turbine engines with comparing its size and lightness, as well as the high percentage of energy that it produces.

The compressor, combustion chamber and turbine blades are the most important components of a turbojet engine and therefore most research focuses on the flow structures of the compressor exit, the outlet temperature field of the combustion chamber and the flow and thermal field around the turbine blades.

The turbine inlet temperature can be increased to achieve peak cycle efficiency, and lower specific fuel consumption [1]. Thus, to achieve the highest possible turbine inlet temperature, accurate knowledge of turbine blade temperatures is required, as frequent excursions beyond the design limits of the blades can significantly reduce service life [2,3].

Gao et al. adopted a variety of methods to reduce the effects of reflected radiation during radiation temperature measurement, determining the value of reflection using the angular radiation factor depending on the position of the turbine blade and the temperature of the adjacent blade by simplifying the blade shapes in two dimensions [4]. Because of the interaction of the blade rows, However,

*Corresponding author.
E-mail address: eng.sipahi@gmail.com (M. Sipahi)
Received 20 November 2022; Received in revised form 11 April 2023; Accepted 01 June 2023

Doi: https://doi.org/10.46460/ijiea.1202422

these analyses are limited by the lack of flow physics as these analyses take place in a very complex rotating machine. The emphasis is placed on the interaction of vortices from the upstream rotor passage with the downstream stator because it causes the nozzle wake velocity defect at the suction surface of the rotor blade [5]. The thermal behavior of the rotor and the flow field are affected when the secondary flow changes downstream of low aspect ratio turbine stages. Based on previous research, a new study published by a group of Indian researchers showed the ideal distances and angles between stator and rotor. Therefore, the distances in this research were relied on this study in order to obtain the best results the ideal angle of burners was 80 degrees, resulting in significant benefits such as lower NOx and CO emissions and overall high combustion efficiency, so this result were relied on this study to obtain better result.

2 Material Method

In this paper ANSYS Fluent Program were used based on the finite element method. The Navier–Stokes equations is used for its ability to solve CFD analysis explicitly which includes a k-ε solver [6-7]. The simulation uses the hybrid solver, which employs an implicit pressure-correction scheme. The SIMPLE algorithm was used to couple the pressure and velocity field [8]. The pressure and temperature data of the combustion chamber obtained from the previous study were used as the initial simulation conditions. The absolute criteria were 1e-6 in the monitors residual [9]. The grids of the computation domain (flow and structure) were created using Solidworks Program. The geometries for conjugated analysis of internal and external heat transfer are shown in Figure. 1-2-3 [10]. The number of meshes needed to calculate the Combustion chamber, Turbine blade is approximately 0.82 million and 0.41 million, respectively as shown in Figure. 4-5. The latter was used to simulate:

1 Kerosene fuel combustion process at combustion chamber.
2 fluid flow and loads on 1.5 stage of turbine blade [11].

The simulations were interdependent on the basis the previous results of combustion process provided data of pressure and temperature distribution, in order to attain physically justified results using CFD analysis.

For the non-premixed burner, a 2D turbulent flow model is used. The non-premixed model solves the transport equation for one or two conserved scalars and the mixture fractions using a modeling approach. There are a variety of chemical species, including radicals and intermediates [12].

The main equations of the gaseous phase model are continuity, the momentum conservation equation, the energy conservation equation, and the chemical component conservation equation.

The computational domain is composed of the combustion chamber and turbine, starting from the compressor's stator exit and ending at the turbine exit [13].

The temperature, pressure and the mass flow rate of fuel and combustion chamber inlet (which is same as in the experiment) is as tabulated below.

Table 1. Properties of initial data.

Flow	Temperature [K]	Pressure [kPa]	Mass flow rate [kgs^{-1}]
Combustion chamber inlet	625.7	1118.2	14.5
Combustion chamber fuel input	353	2757	0.4
Turbine inlet	1700	2138.8	14.9

In the analysis process meshing of the gas turbine blade is done using finite element analysis. The meshing information of Combustion chamber and turbine blade are shown in Table 2.

In this study, a tetrahedral mesh was chosen, which has the benefit of being able to well approximate the surface contour, to get good results [14]

.

Table 2. Mesh modeling data.

Parameter / Domain	Combustion chamber	Turbine
Meshing method	Triangles	Triangles
Total elements	823918	414083
Total nodes	486209	245334

The distance between stator and rotor is given Xs Axial spacing =25% depending on previous research as viewed at Figure 3 [11]. The front, side, elevation and isometric projections of the GE90 engine are shown in Figure 1.

The side projection of the combustion chamber section and nacelle without turbine section are shown in Figure 2.

The side projection of the turbine blade section for 1.5 stage of (rotor-stator-rotor) and nacelle are shown in Figure 3 [11].

The combustion chamber section and nacelle after mesh process are shown in Figure 4. The mesh process was concentrated at the fuel outlet and nozzle in order to obtain better results in the CFD process. [15].

The Turbine blade section for 1.5 stage of (rotor-stator-rotor) after mesh process are shown in Figure 5. The mesh process was applied equally to all parts of the turbine in order to obtain better result in the CFD process.

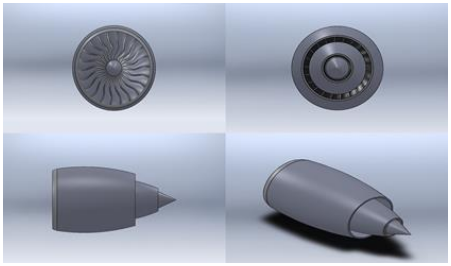

Figure 1. Design of engine nacelle model.

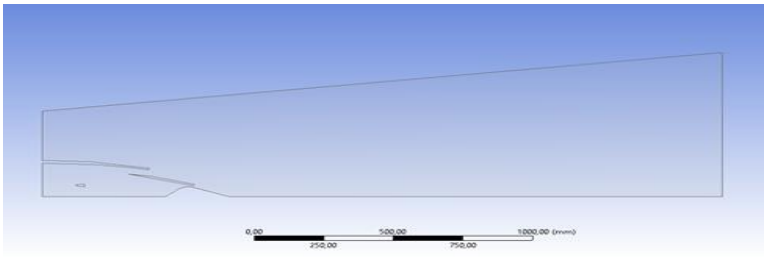

Figure 2. Information about simulation conditions for combustion chamber.

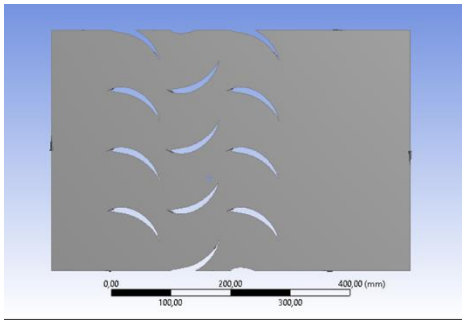

Figure 3. Information about simulation conditions for 1.5 stage turbine blade.

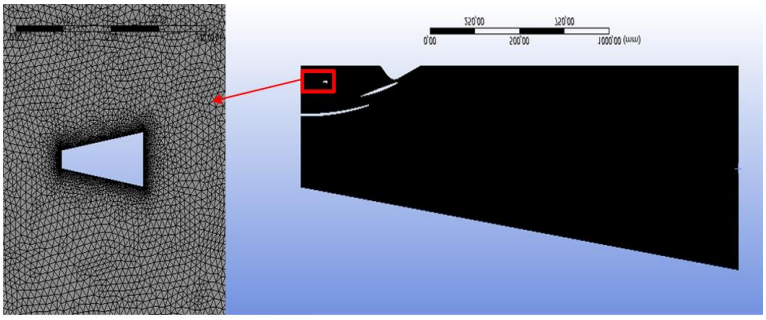

Figure 4. Mesh for combustion chamber.

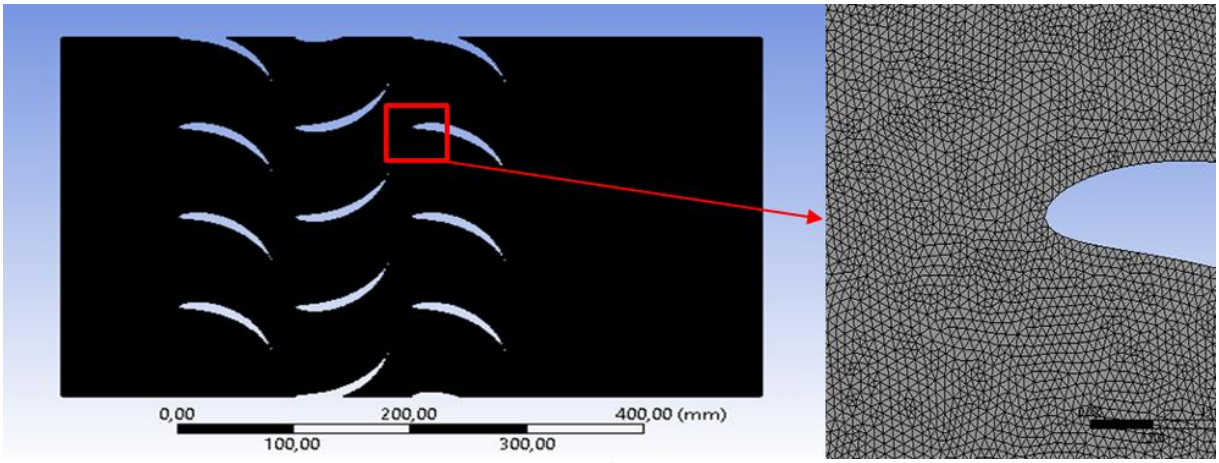

Figure 5. Mesh for turbine blade.

3 Analysis and Result

It's clear that the continuity equation, the energy preservation equation and the momentum conservation equation are the basic equations of the phase of gaseous models. Figure 6 shows the temperature contours of kerosene and oxygen mixture inside a combustion chamber. The high temperature zones are completed faster because kerosene fuel provides the processes of fuel combustion. Because of the progressive evaporation and burning of the used fuel within the combustion chamber in predetermined streams in causes the flame concentration to rise as the fuel amount rises. Moreover, it is known that the peak temperatures of the burning fuel inside the combustion chamber are in the range of 2200-2700 K, and for our model it can be seen that the peak temperatures in the cross-section's length of the combustion chamber are in the range of 1200–2000 K.

It is important to remember that the formula determines the coefficient of the average temperature filed non-uniformity.

$$\delta = \frac{T_{max} - T_{min}}{T_{av}} \quad [16] \qquad (1).$$

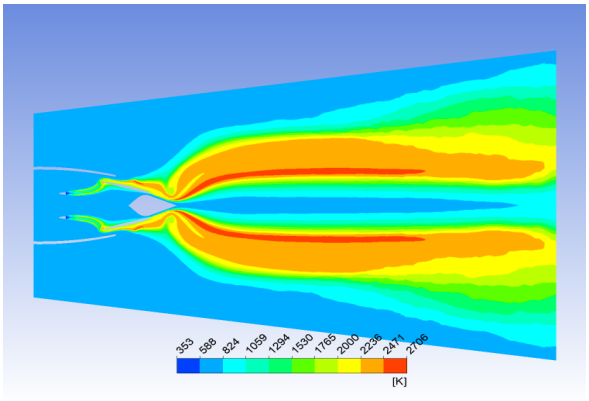

Figure 6. The temperature contour distribution after burning.

Figure 7 shows the distribution of the masses of oxygen and carbon dioxide in the cross-section of the combustion chamber along specific paths. The high amount of oxygen can be observed in local areas located behind the outer swirler, and the proportion of carbon dioxide in the outer swirler has increased in because of the burning fuel.

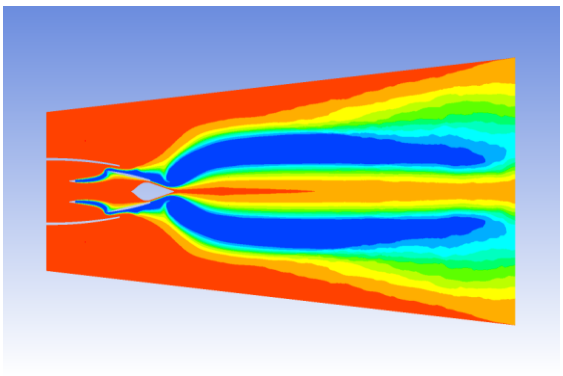

Figure 7. The mass fraction of CO2 and O2.

The pressure distribution in the blade pitch diameter portion at different flow rates is shown in Figure 8. The outcomes of the numerical simulation demonstrate that, regardless of the flow rate, the pressure gradient variation trend in the calculation domain is practically the same. High temperature working fluid arrives from the inlet section and flows through the stator blade, as seen by the image of the pressure distribution cloud. As a result of leaving the rotor blade runner, the working fluid's pressure becomes lowers. The rotor blade's working face is under intense pressure, while the non-working face is under minimal strain. The pressure gradient increases as a result of the uneven flow of the working fluid when it enters the rotor blade runner. As soon as the high temperature working fluid exits the stator blade, it rapidly expands. Because the energy loss is lower in accelerated gases flow, the numerical simulation results demonstrate that the working fluid accelerates as it leaves the rotor blade runner. [17].

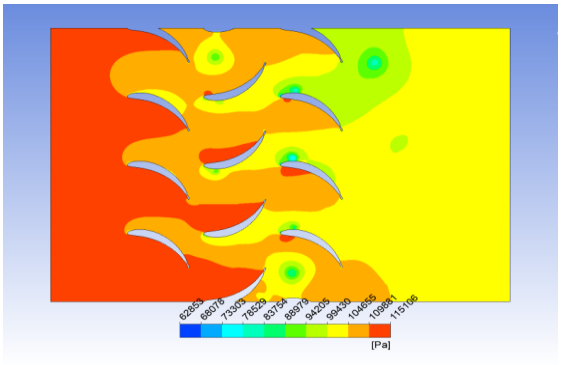

Figure 8. The Pressure for turbine blade.

The flowing fluid flows between the stator blades (stational blades) and the rotor blades (rotation blades). The stator and rotor pitch diameters of the gas turbine are depicted in Figure 9 together with the velocity distribution of the flow field. As seen in the model given in Figure 9, the working fluid enters the stator blade at high temperatures and low velocity. Meanwhile, the carbon particles collide with the fins together with the work fluid. The high velocity working fluid coming out of the stator blade hits the rotor blade, and then some of the working fluids entering the rotor blade runner hit the rotor blades at low speeds. The first blades from the left are stator blades, this stage is called the impulse stage and all the pressure drop in stational blades takes place at this stage, the pressure remains constant in the flow through the blades. The middle fins are rotor blades, when there is a pressure drop across the stator and rotor blades in the reaction stage, leakage occurs at the tips of the blades, but it is observed in the model that the leaks at the blade tips are controlled.

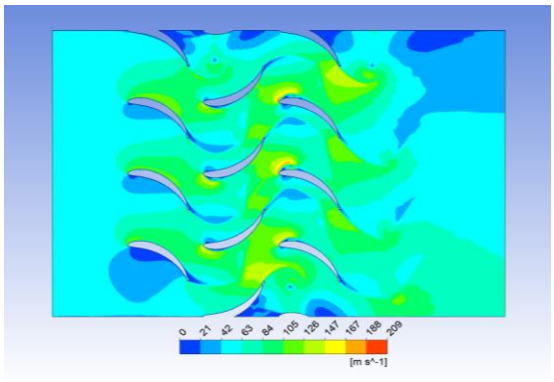

Figure 9. The Velocity for turbine blade.

The distribution of carbon particles in the rotor blade under various flow rate conditions is shown in Figure 10. The carbon particles collide with the rotor blades due to the separate or combined effects of working fluid the turbulence of the high temperature, the inertia forces, the thermophoresis forces, and other factors and the carbon particles flow over the stator blades together with the high temperature working fluid. As highlighted also by G.Liu et al. [18]. the working fluid accelerates with the movement of the stator blade and hits the rotor blade at high velocity but some of the carbon particles by enter the rotor blades runner hit the rotor blades at low speeds and move away from the rotor blades at high velocity with together the high temperature working fluid. It can be observed that the working fluid velocity gradually increases and moves towards higher radius depending on the increase in tangential velocity between turbine stages.

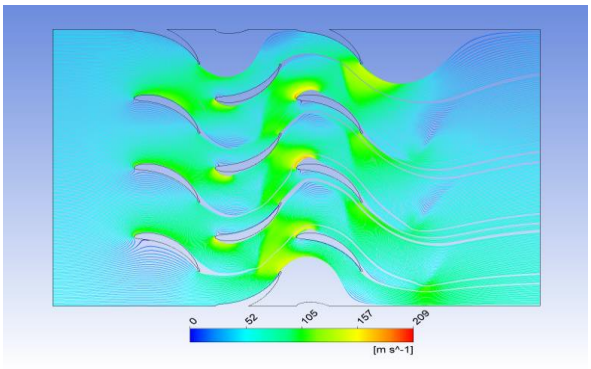

Figure 10. The Streamline for turbine blade.

4 Conclusion

Combustion occurs mostly before the gas reaches the stator's leading edge. Along the stator channel, the hot gases mix with the main flow. The flow variables for steady cases are noted, such as velocity and pressure profiles. Under steady flow conditions, the pressure distribution along the blade passage shows a high pressure over the first blade surface and decreases towards the outlet. At the inlet of each rotor stage, a highly uniform temperature distribution is achieved.

The pressure and velocity behaviors of the working fluids flowing between the stator and rotor blades of the gas turbine were investigated with the numerical analysis. The results obtained here will lead to. After the working fluid enters the stator blades, the pressure of the fluid turns into kinetic energy and does work by striking the rotor blades. At the same time, the carbon particles in the working fluid will increase the wear due to impact. The greatest pressure occurred on the inner surface of the stator blade. In the numerical analysis results, it is seen that there is a significant acceleration when the work fluid flows from the rotor blades and the work fluid at high temperature starts at low velocity. The high temperature working fluid entering the stator expands by converting its heat and pressure energy into kinetic energy.

Acknowledgements

This study is related to the corresponding author's MSc research.

Declaration

Ethics committee approval is not required.

References

[1] Kerr, C., & Ivey, P. (2002). An overview of the measurement errors associated with gas turbine aeroengine pyrometer systems. *Measurement science and technology*, 13(6), 873.

[2] Willsch, M., Bosselmann, T., & Theune, N. M. (2004, October). New approaches for the monitoring of gas turbine blades and vanes. In *Sensors*, 2004 IEEE (pp. 20-23). IEEE.

[3] Horlock, J. H., & Torbidoni, L. (2006). Turbine blade cooling: the blade temperature distribution. *Proceedings of the Institution of Mechanical Engineers, Part A: Journal of Power and Energy, 220(4)*, 343-353.

[4] Gao, S., Wang, L., Feng, C., Xiao, Y., & Daniel, K. (2015). Monitoring temperature for gas turbine blade: correction of reflection model. *Optical Engineering*, 54(6), 065102-065102.

[5] Pullan G (2006). Secondary flows and loss caused by blade row interaction in a turbine stage. *ASME Journal of Turbomachinery* 128:484–491.

[6] Chaluvadi VSP, Kalfas AI, Hodson HP, Ohyama H and Watanabe E (2003). Blade row interaction in a high-pressure steam turbine. *ASME Journal of Turbomachinery* 125:14–24.

[7] Serbin, S., Diasamidze, B., Gorbov, V., & Kowalski, J. (2021). Investigations Of the Emission Characteristics Of A Dual-Fuel Gas Turbine Combustion Chamber Operating Simultaneously On Liquid And Gaseous Fuels. *Polish Maritime Research*, 28, 85-95.

[8] Lei, Z., & Ting, W. (2012). Computational Fluid Dynamics Guided Investigation for Reducing Emissions and Increasing Exergy of the Pyroscrubber in a Petcoke Calcining Facility. *Journal of Thermal Science and Engineering Applications*, 4(1).

[9] Shankar, K. S., Ganesh, M., & Kumar, K. S. (2018, December). Combustion Chamber Analysis Using CFD for Operation Condition. In IOP *Conference Series: Materials Science and Engineering* (Vol. 455, No. 1, p. 012032). IOP Publishing.

[10] Samarasinghe, T., Abeykoon, C., & Turan, A. (2019). Modelling of heat transfer and fluid flow in the hot section of gas turbines used in power generation: A comprehensive survey. *International Journal of Energy Research*, 43(5), 1647-1669. 2018.

[11] Babu Ummiti, M., Sitaram, N., & Prasad, B. V. S. S. S. (2009). Computational investigation of effect of axial spacing on blade row interaction in a 1½ stage axial flow turbine. *Engineering Applications of Computational Fluid Mechanics*, 3(1), 56-70.

[12] Zadghaffari, R., Moghaddas, J. S., & Rahimiahar, Z. (2012). Numerical investigation of a burner configuration to minimize pollutant emissions. *APCBEE Procedia*, 3, 177-181.

[13] Mangra, A. C. (2020, September). Micro gas turbine combustion chamber CFD modelling. In IOP Conference Series: *Materials Science and Engineering* (Vol. 916, No. 1, p. 012064). IOP Publishing.

[14] Mehmert, P. (2023). Residual stress analysis and geometrical tolerances in powder bed fusion and direct energy deposition processes. In *Quality Analysis of Additively Manufactured Metals* (pp. 429-486). Elsevier.

[15] Sharma OP, Pickett GF, Ni RH (1992). Assessment of unsteady flows in turbines. *ASME Journal of Turbomachinery* 114:79–90.

[16] Benim, A. C., Iqbal, S., Meier, W., Joos, F., & Wiedermann, A. (2017). Numerical investigation of turbulent swirling flames with validation in a gas turbine model combustor. A*pplied thermal engineering*, 110, 202-212.

[17] Fakheri, F., Moghaddas, J., Zadghaffari, R., & Moghaddas, Y. (2012). Application of central composite rotatable design for mixing time analysis in mechanically agitated vessels. *Chemical engineering & technology*, *35(2)*, 353-361.

[18] Liu, G., Sun, S., Liang, K., Yang, X., An, D., Wen, Q., & Ren, X. (2021). Simulation study on the effect of flue gas on flow field and rotor stress in gas turbines. *Energies*, 14(19), 6135.